Air Gasification of Biomass in a Downdraft Fixed Bed: A Comparative Study of the Inorganic and Organic Products Distribution

I. De Bari,* D. Barisano, M. Cardinale, D. Matera, F. Nanna, and D. Viggiano

*Biomass Laboratory, Renewable Energy Division, ENEA, Italian Agency for New Technology,
Energy and Environment, Policoro (MT) 75025, Italy*

This paper deals with the gasification of agricultural residues such as almond shells and wood at high temperature (850 °C) in a small-scale gasification plant coupled with a reciprocated internal combustion engine. Detailed investigation of both organic (tar) and inorganic (NH_3, HCN, metals, etc.) products distribution in the process streams are provided. This research aims to assess the existence of certain relations between feedstock composition and the observed products distribution in the steady state. Biomass feedstock is characterized for its elemental composition, its content of metallic species, and lignin, cellulose, and hemicellulose fractions. A different feedstock composition was found to be associated with some important variations in the process monitored parameters such as the gasification rate, the tar content, and the char yield in the flue gas. Also a relation was found between the relative amount of ammonia and cyanide species in the flue gas at the operating conditions of the gasifier (oxygen-to-biomass ratio and activated carbon support). Spectroscopic features of the sludgy condensate formed in the upper part of the gasifier during the early stage of the process together with the characterization of char, fly ash, and acidic species in the flue gas shed light on some mechanistic aspects of the gasification process.

Introduction

Gasifying agricultural residues is a promising option especially in view of electricity production. Biomass gasification is a complex thermochemical process that converts lignocellulosic materials into a valuable gas by means of a partial oxidation process at high temperature. The gas mixture from the process can be utilized to produce electrical energy and thermal power, giving a positive contribution in terms of energetic and environmental policies.

Under typical gasification conditions, the gas composition mainly consists of CO (18–21%), H_2 (10–16%), O_2 (1.5–2.5%), CH_4 (1–3%), and N_2 (40–54%) together with traces of hydrocarbons (ethane, etc.), volatile ash, organic condensable compounds (tar), and inorganic constituents such as HCN, NH_3, whose burning causes high nitrogen oxide emissions. In the past, considerable research has been carried out to study how the exact composition of the produced tar at the gasifier exit varies as a function of gasifier geometries[1] and processing variables.[2] Most recent research studies on the chemistry of tar formation from biomass have pointed out the existence of a dependence of tar yields from both the temperature and the type of feedstock loaded.[3] Gas temperature and fuel chemical composition also play a

decisive role in determining the amount of nitrogen compounds (NH_3 and HCN) in the flue gas[4] as well as the ash composition and volatilization during the gasification process.[5] Better knowledge of the tar evolution and the fate of inorganic constituents of the flue gas has highlighted the importance of studying the analytical framework of the gasification process in order to improve the process technology by choosing tailored strategies, including biomass pretreatment and gas cleaning.[6]

Despite the scientific and technical knowledge gained about the contaminants embedded in the flue gas, to date, very little attention has been devoted to the relation between the initial composition of the biomass feedstock (both in its organic and inorganic constituents) and the minor products at the exit of the gasifier or among the process products themselves. To the best of our knowledge, only a few papers have dealt with the action of inorganic constituents in the biomass as

---

* To whom correspondence should be addressed. Fax: +39 0835-974210. E-mail: de_bari@trisaia.enea.it.
(1) Rajvanshi, A. K. Biomass Gasification. *Alternative energy in agriculture*; CRC Press: Boca Raton, FL, 1986; Vol. 2, pp 83–102.
(2) Kinoshita, C. M.; Wang Y.; Zhou J. Tar Formation Under Different Biomass Gasification Conditions. *J. Anal. Appl. Pyrolysis* **1994,** *29,* 169.

(3) Brage, C.; Qizhuang, Y.; Guanxing, C.; Sjöström, K. Tar Evolution Profiles Obtained from Gasification of Biomass and Coal. In *Biomass for Energy and Industry, Proceedings of the International Conference Würzburg*; Kopetz, H., Weber, T., Palz, W., Chartier, P., Ferrero, G. L., Eds.; C.A.R.M.E.N.: Germany, 1998; pp 1634–1637.
(4) Leppälahti, J. Formation and Behaviour of Nitrogen Compounds in an IGCC Process. *Bioresour. Technol.* **1993,** *46,* 65–70.
(5) Baxter, L. L.; Miles, T. R.; Miles, T. R., Jr.; Jenkins, B. M.; Milne, T.; Dayton, D.; Bryers, R. W.; Olden, L. L. The Behavior of Inorganic Material in Biomass-Fired Power Boilers: Field and Laboratory Experiences. *Fuel Process. Technol.* **1998,** *54,* 47–78.
(6) Hasler, P.; Buhler, R.; Nussbaumer, T. Evaluation of Gas Cleaning Technologies for Biomass Gasifiers. In *Biomass for Energy and Industry, Proceeding of the International Conference Würzburg*; Kopetz, H., Weber, T., Palz, W., Chartier, P., Ferrero, G. L., Eds.; C.A.R.M.E.N.: Germany, 1998; pp 272–275.

---

indigenous catalysts toward biomass pyrolysis and gasification reactions.[7-9] In particular, DeGroot and Richards[8] observed that the gasification of char would occur more quickly in the presence of a higher metal ion content (alkali and alkaline earth metals), while Agblevor and Besler[10] concluded that the inorganic constituents in the biomass act as nucleation centers toward the char formation. Moreover, literature data about the evolution of the inorganic species NH_3 and HCN mainly concern coal and peat,[11-14] and less data are available on agricultural residues gasification on small-scale fixed bed plants.

This paper describes the fate of both organic and inorganic constituents during the gasification of biomass in a fixed bed gasifier, shedding new light on the chemistry involved in this biomass processing, and explores how the organic and inorganic fuel constituents could influence each other during the process. Finally, an attempt at describing HCN and NH_3 behavior as a function of the feedstock loading and the gasification ratio (air−fuel ratio) is performed.

Comprehensive test runs were carried out in a fixed bed downdraft gasifier using some common European biofuels (oak, turkey oak, almond shells). The gasification of lignocellulosic residues by means of such simple and versatile plants is dictated by the necessity of developing technologies capable of processing different biomass feedstocks for small-scale power production (e.g. agroindustries and remote zones). The employed biomass was characterized for its inorganic constituents, sugars, extractives, and lignin content, while a detailed analysis of products from plant running was carried out following a suitable gas sampling.

The available standard methods for fuel analysis mainly concern coal and coke. In recent years, with increasing interest in the energetic valorization of biomass, some laboratories[15] cooperate in trying to establish a best practices list for biomass fuel and ash analysis by selecting and adapting the available standard methods. Hence, as there are not yet standardized methods available for sample preparation and analysis of biomass fuels and ashes, optimized analytical proce-

dures were developed in our laboratories in order to determine the feedstock composition as well as the constituents embedded in the flue gas. In this work several analytical techniques were used to get a more complete picture of the formation of products from gasification of certain biomass.

Experimental Section

Pilot Plant Used. All the experiments were carried out on a 120 kW$_{th}$ gasifier which operates in downdraft mode utilizing air as the gasifying agent. Scheme 1 reproduces the major components of the gasification plant used. The plant core (Scheme 2) is a double wall cylindrical chamber whose combustion zone is made of stainless steel with a double conic shape. The inner part of this zone contains a plane with nozzles. The double chamber compensates for heat loss and allows a preheating of biomass. The cleaning section consists of four filtration stages: cyclone filter, scrubber filter, demister system, and chips filter. The utilization section contains a power unit equipped with a gas fueled modified FIAT diesel engine coupled with a 25KVA alternator. The generated power is consumed by means of electric resistances placed in a water bath. The maximum consumable power is 24 kW, and the effective utilized power can be varied between 1 and 24 kW by 1 kW steps. In particular, during our experiments the dissipated power was settled at 21 kW. The gasifier was operated at a temperature of about 850 °C. Air was fed into the gasifier at an average flow rate of 36 N m³/h.

Sampling. Gas sampling was performed isokinetically according to a geometry reproduced in Scheme 3. This geometry was evaluated to be the most suitable to ensure the collection of the flue gas main constituents. The gas mixture was automatically sampled with a flow rate of 5 L/min. To avoid high molecular weight tar deposition, a heating element prior to the particles collector ensured a middle temperature of almost 200 °C. The organic and inorganic samplings were executed separately to avoid any fouling of the sampling system caused by the solidification of water from the inorganic solutions on the dichloromethane collecting solution. With regard to the tar sampling, gas was bubbled in a five washing bottles system filled with dichloromethane. The first two bottles were cooled in an ice bath while the last ones were cooled in a −10 °C thermostatic bath. Only fresh solutions were considered for tar analysis in order to avoid any modification in composition caused by repolymerization reactions or evaporation of organic solvent. A three bottles system was employed to collect the inorganic species embedded in the flue gas. The acidic constituents were determined by collecting the flue gas on Na_2CO_3/$NaHCO_3$ (2.7 mM/0.3 mM), while ammonia was collected onto a 5 mM H_2SO_4 solution. Both solutions were cooled at 0 °C. The collecting equipment was previously rinsed with abundant bi-distilled water and finally rinsed with the collecting solution. All the concentrations were normalized for the collected gas volume referred to normal conditions.

Slugging material was also collected from the upper part of the gasifier in order to evaluate its chemical composition.

Three different plant zones were chosen for the ammonia content evaluation: (1) after the glass filter; (2) in the scrubber solution; (3) in the condensed phase onto the chips filter.

Analyses of Anions. To determine elements of interest in the tested biomass and in the flue gas, ion chromatography analyses with a HPIC DX 300 system were performed. Accurately weighed biomass samples of approximately 0.3 g were first combusted in 30 bar oxygen using a Malher bomb (ISO-587, ASTM 2361-66). The solutions containing the anions from biomass (Cl, S) were then eluted through an AS 12 ionpac column. Tests on several standards including 3-chlorine, 4-fluorine aniline, and bromothymol blue showed reproducible recoveries of almost 90% for chlorine and 60% for sulfur species.

(7) DeGroot, W. F.; Richards, G. N. Influence of Pyrolysis Conditions and Ion − Exchange Catalysts on the Gasification of Cottonwood Chars by Carbon Dioxide. *Fuel* **1988**, *67*, 352−360.

(8) DeGroot, W. F.; Richards, G. N. The Effect Influence of Ion-Exchanged Cobalt Catalysts on the Gasification of Wood Chars by Carbon Dioxide. *Fuel* **1988**, *67*, 345−351.

(9) DeGroot, W. F.; Kannan, M. P.; Richards, G. N.; Theander, O. Gasification of agricultural residues (biomass): Influence of inorganic constituents. *J. Anal. Appl. Pyrol.* **1984**, *38*, 320−323.

(10) Agblevor, F. A.; Besler, S. Inorganic Compounds in Biomass Feedstocks. 1. Effect on the Quality of Fast Pyrolysis Oils. *Energy Fuels* **1996**, *10*, 293−298.

(11) Leppälahti, J.; Kurkela, E. Behaviour of Nitrogen Compounds and Tars in Fluidized Bed Air Gasification of Peat. *Fuel* **1991**, *70*, 491−497.

(12) Leppälahti, J.; Kurkela, E.; Simell, P. Catalytic Conversion of Nitrogen Compounds in Gasification Gas. *Fuel Process. Technol.* **1991**, *29*, 43−56.

(13) Leppälahti, J. Formation of NH_3 and HCN in slow-heating-rate inert pyrolysis of peat, coal and bark. *Fuel* **1995**, *74*, 1363.

(14) Leppälahti, J.; Koljonan, T. Nitrogen Evolution from Coal, Peat and Wood During Gasification: Literature Review. *Fuel Process. Technol.* **1995**, *43*, 1−45.

(15) Best practices list for biomass fuel and ash analysis; ECN, Report No. ECN-C-98-0875; Netherlands Energy Research Foundation: Petten, The Netherlands, 1998.

(16) Sander, M. L.; Ericsson, T. Vertical Distributions of Plant Nutrient and Heavy Metals in Salix Viminalis Stems and Their Implications for Sampling. *Biomass Bioenergy* **1998**, *14* (1), 57−66.
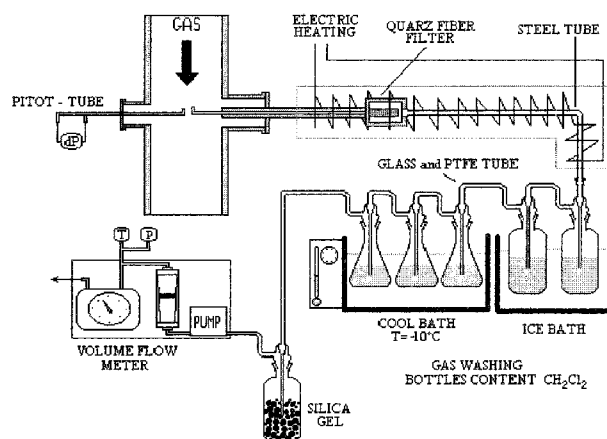
Scheme 1. Fixed Bed Gasification Plant Used[a]
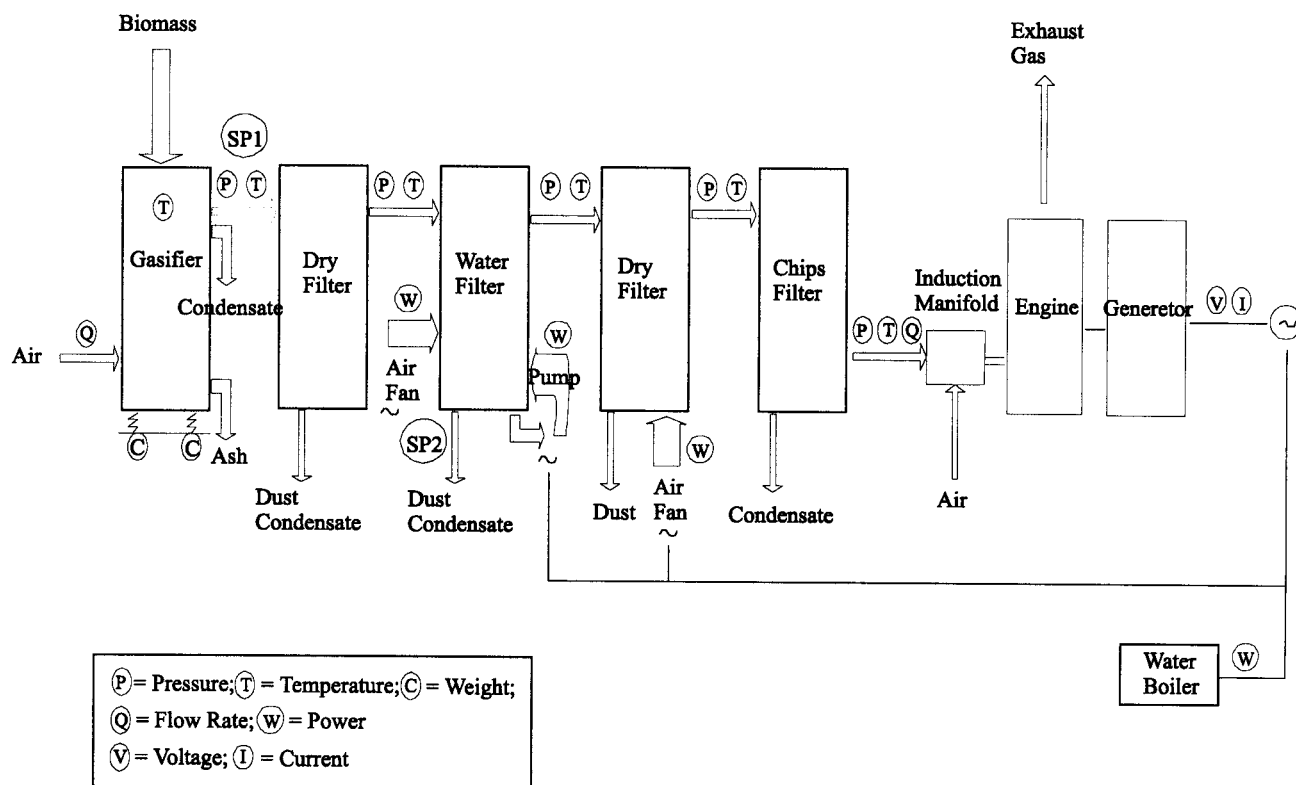
[a] In the scheme are also indicated the flue gas sampling points (SP1 and SP2).

Scheme 2. Fixed Bed Gasifier
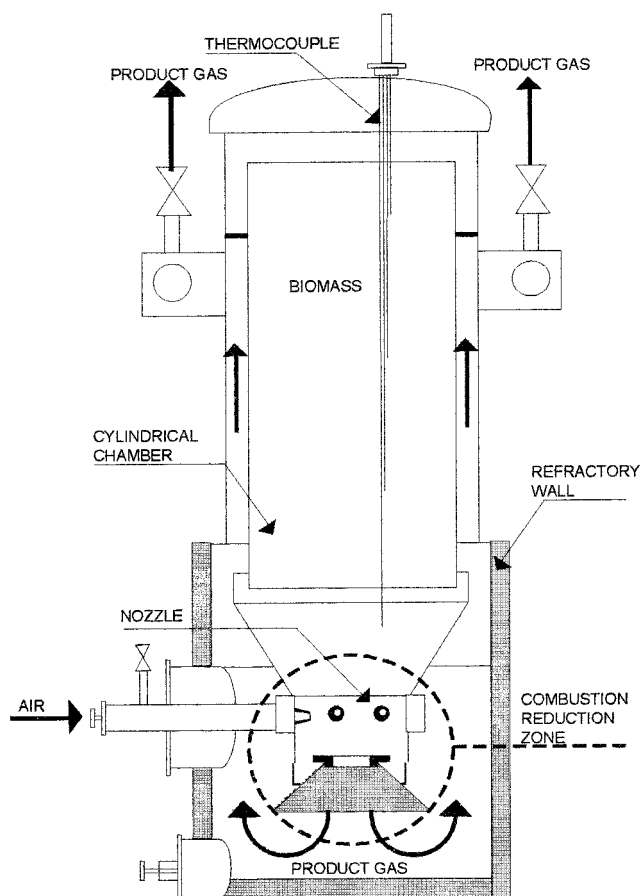
The $Na_2CO_3/NaHCO_3$ collecting solutions from plant runs were analyzed for their content in the following anions: Cl^-, NO_2^-, NO_3^-, SO_4^{2-}, PO_4^{3-}, CH_3COO^- (acetates), and $HCOO^-$

Scheme 3. Equipment Adopted for Tar Sampling[a]

[a] Analogous equipment was used for inorganic sampling with the exception of the $- 10\ °C$ section.

(formiates). An eluting mixture of $Na_2CO_3/NaHCO_3$ (2.7 mM/0.3 mM) was selected to separate Cl^-, NO_2^-, NO_3^-, SO_4^{2-}, and PO_4^{3-}, while an eluting mixture of $B_2O_7^{2-}/NaOH$ (75 mM/100 mM) was shown to be suitable to discern the contribution from formiates and acetates. Identification and quantification were performed by comparison of retention times and responses with those of standard solutions.

FTIR Mesurements. The sludgy condensate collected in the upper part of the gasifier was subjected to several treatments to obtain samples easy to handle. In this regard, several solubilization procedures were evaluated. The more effective one provided a preliminary treatment with an alkaline solution 1 N to separate the polar from the hydrophobic fraction. Mass balance estimations revealed that the solid hydrophobic fraction separated in this way is at least 1% of the collected material, and the FTIR spectrum indicated the char features of this fraction. The basic solution was then acidified with 1 N H_2SO_4 until pH 2 was reached. In this

Table 1. Elemental Composition (wt %) and Fixed Carbon on Dry Matter of the Three Biomass Feedstocks

feedstock	C	H	O	N	S	Cl	fixed carbon
almond shells	45.0	5.0	48.0	0.40	0.0170 ± 0.0012	0.0100 ± 0.0005	16.32
oak	50.0	6.0	43.0	0.10	0.027 ± 0.005	0.04 ± 0.01	14.39
turkey oak	50.0	6.0	43.0	0.10	0.101 ± 0.005	0^a	15.22

[a] Only trace elements were detected, and the relevant signals were below the determinability limits.

condition a solid material precipitated. Following filtration on a glass fiber filter, this material was collected, dried in an oven at a temperature of 90 °C for 4 h, and then used to prepare KBr pellets in less than 1wt % concentration. IR spectra were recorded with a Perkin-Elmer 2000 spectrometer in the transmission mode, adopting a resolution of 2 cm^{-1}. Spectra were also recorded in ATR mode. No significant differences were observed.

Elemental Analysis (C, H, N, O) and Fixed Carbon. For the determination of the elemental composition a Perkin-Elmer 2400 multielement analyzer was employed. Approximately 3−4 mg of dried and pulverized sample was weighed with an accuracy of 0.01 mg and placed in an aluminum container. Helium was used as carrier gas.

Fixed carbon was determined according to ASTM D3175 and D3172 standard procedures.

Ash Determination. Ash determination was performed with a sample of ca. 1 g in a furnace according to ASTM D1102.

Extracts, Lignin, and Carbohydrates. The samples (ground at 50 mesh and dried to 105 °C) were extracted in a Soxhlet with an ethanol/toluene (1/2) solution for 7 h. This procedure (ASTM D1106, D1107, D1108) ensured the extraction of resins, fats, wax, oils, and catechols. The percentages of the extracts were referred to the dried biomass.

Lignin quantification was performed on the samples previously extracted with the ethanol/toluene mixture. The amount of Klason lignin was quantified according to the Mod. Tappi T-13 m-54 and ASTM D1106 standard method. The samples were treated with concentrated sulfuric acid (72% (w/w)). The relevant solution was then diluted (3%), heated until it reached ebullition, and kept in ebullition for 4 h at constant volume. An insoluble residue of lignin (Klason lignin) was obtained. Its percentage composition was referred to the dry matter with the extractives.

The acidic solution obtained from the previous step was analyzed by means of a HPIC DX 300 equipped with a Carbopac 100 column in order to evaluate the total amount of carbohydrates. The analytical results were corrected with experimental factors to account for the sugars degradation occurring during the hydrolysis step.

Analysis of Heavy and Alkali−Alkaline Earth Metals. The metal content of the biomass used was established on ground and homogenized samples digested in ACV closed vessels (volume, 100 mL) with a mixture of HNO$_3$/HF (10:1). Quartz filters from the plant were combusted in a muffle operating at 600 °C to completely remove the organic fraction (char). The inorganic fraction was then subjected to microwave digestions in ACV closed vessels. The acid volume used in the digestion procedure was a mixture of 10 mL of HNO$_3$ and 15 mL of HF. The digestion temperature was almost 180 °C, and the duration of the mineralization procedure was 40 min. Digestion of two blank filters was also executed under the same conditions of the samples in order to evaluate the contribution from the collecting medium. The digestions were performed with a CEM-2000 oven equipped with both a pressure and a temperature control unit. Prepared inorganic samples were analyzed in a Varian Ultramass ICP-MS spectrometer. Before the determination, samples were diluted 500 times. Samples were stored in bottles made of PC preliminarily conditioned in a 20% HNO$_3$ solution and then abundantly rinsed with bi-distilled water.

Ammonia Determination. The ammonia content was determined according to the Nessler method. Aqueous solu-

Table 2. Mean^a Trace Metal Contents (mg/Kg in ash) of Three Different Biomass Feedstocks

	feedstock		
metal	almond shells	oak	turkey oak
Na^b	5.8	4.0	4.3
Mg^b	10.7	12.6	12.28
Al^b	3.7	0.56	2.66
K^b	330	38	65
Ca^b	55	250	400
Fe^b	3.6	9.0	10.79
Cd	4.0	3.9	3.2
Cr	740	194	345
Cu	490	172	105
Mn	540	980	Nd
Ni	1220	340	450
Pb	2000	269	260
Zn	3700	1180	2020

[a] Data reported for alkali and heavy metals are affected by two sources of errors: the variance within-sample and the variance between samples. The first values are usually negligible (0.5%), while the second values are of the order of 10%. This result could be explained by taking into account that plant nutrient and heavy metal concentration could vary along the wood trunk.[16] [b] Relevant amounts are divided for 10^3.

tions from the wet scrubber were first filtered on an activated carbon bed to remove the organic species, making the solution look colored, and subsequently analyzed according to the standard procedure (ASTM D1426-79).

Cyanide Determination. The cyanide content of the flue gas was determined on the collecting basic water solution by means of ionic chromatography. A solution of C$_2$O$_4^{2-}$/NaOH (7.5 mM/0.2 mM) was used to isocratically elute samples through a Carbopac 100 column. The employed electrochemical detector was an ED40 silver working electrode anodically polarized at 0.1 V.

Sample Preparation for GC-MS Analysis. Tar solution from the plant was placed in a separator funnel to allow water-phase separation. With the exception of a few runs no significant amount of the water phase condensed onto the dichloromethane solution. Prepared tar samples were analyzed in a HP 6890 GC-MS. A HP-5MS (cross-linked 5% PH ME siloxane, 30 m × 0.25 mm × 0.25 μm film thickness) column was used for tar analysis. GC analysis provided an exploration of the mass region from 35 up to 300 amu. Identification of each component was based on the analyte retention times from a certified mixture of polynuclear aromatic hydrocarbons (EPA 610 calibration standard, Supelco Inc.), BETX, and phenol standards (certified by ULTRA Scientific). Also, the quartz filters used to collect particulate were extracted for 2 h with dichloromethane in a Soxlet apparatus to evaluate the presence of aromatic compound on the particulate by means of GC-MS analysis. The obtained results showed no presence of tar traces on the quartz filter.

Materials. The acids used in the digestion of biomass samples were HNO$_3$ (70%, E. Merck, suprapur) and HF (40%, E. Merck, suprapur). All other chemicals were of analytical grade. Biomass samples for chemical characterization were prepared by first grinding a significant amount of biomass and then subsampling for analysis.

Surface Area Measurements. Multipoint BET analyses of surface area were determined by N$_2$ adsorption at −6 °C using a Quantacrom Nova 2200 apparatus.

Table 3. Sugar Percentages into the Three Biomass Feedstocks

	araban	galactan	glucan	xylan	cellobian[a]
almond shells	1.31 ± 0.13	1.12 ± 0.11	23 ± 2	33.09 ± 1.1	2.08 ± 0.08
oak	1.18 ± 0.12	1.13 ± 0.14	32.8 ± 1.3	23.7 ± 1.8	2.21 ± 0.19
turkey oak	1.24 ± 0.12	1.45 ± 0.17	33.0 ± 1.8	23.1 ± 1.3	2.6 ± 0.2

[a] The cellobian in the analyzed solution is due to an incomplete hydrolysis of the cellulose backbone.

Table 4. Percentage Composition of Three Biomass Feedstocks[a]

	sugars	lignin	ash[b]	extractives[c]
almond shells	60.6	29.0 ± 1.2	1.38	2.9
oak	61.02	24.4 ± 0.4	2.13	5.6
turkey oak	61.39	23.0 ± 0.5	2.17	4.3

[a] Data reported are referred to the biomass dried at 105 °C. [b] The reported results are affected by standard errors of 5%. [c] This extractives percentage comprises compounds such as resins, fats, wax, oils, and cathecols. The reported results are affected by errors of 7%.

Results and Discussion

Characterization Analysis of Biomass Residues. Table 1 summarizes the elemental composition (C, H, O, N, S, Cl) and the fixed carbon content of the three biomass feedstocks loaded, while Table 2 gives the relevant metal compositions. The results reported in Tables 1 and 2 suggest immediately that alkali metals in the biomass matrix cannot be only like inorganic salts such as KCl. In fact, the potassium concentration in the analyzed biomass is at least 1000-fold the chlorine concentration.

The presence of appreciable amounts of heavy metals (Cd, Ni, etc.) extraneous to the indigenous composition of the tested biomass could be due to a biosorption process which might involve the carboxyl, the amine, and the amide groups of the biomass. The comparison of the biomass compositions detailed in Table 2 suggest that while oak and turkey oak show a quite similar inorganic composition, almond shells are different. In particular, it is immediately evident from the data reported above that calcium, which is likely to be predominantly present in cell wall material, is more abundant in woody biomass compared to almond shells. An opposite result was found for potassium ion.

Table 3 is a compilation of the detailed composition of the measured sugar content in the tested biomass, while Table 4 includes the percentages of the other constituents. Considering that summary was affected by an error of at least 10%, the mass balance for the analyzed biomass can be considered to be almost 100%. On the basis of these results, it can be concluded that although woody biomass and almond shells contain a comparable amount of sugars, the content of the most abundant components, glucan and xylan, is almost inverted by passing from woody biomass to almond shells. Other differences reside in the lignin and ash content. In particular almond shells contain higher lignin content than the analyzed woody biomass, while they give a lower ash yield. The observed difference in the lignin content is also consistent with the recorded FTIR spectra of the dried raw biomass shown in Figure 1. In particular, useful indications about the holocellulose (cellulose and hemicellulose) to lignin ratio can be deduced by measuring the intensities ratio of the absorption bands at 1738 and 1510 cm^{-1}, respectively
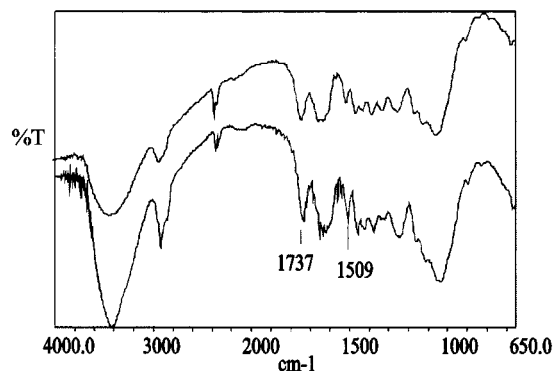

Figure 1. FTIR spectra acquired from turkey oak (upper curve) and almond shell (lower curve) dried raw material.
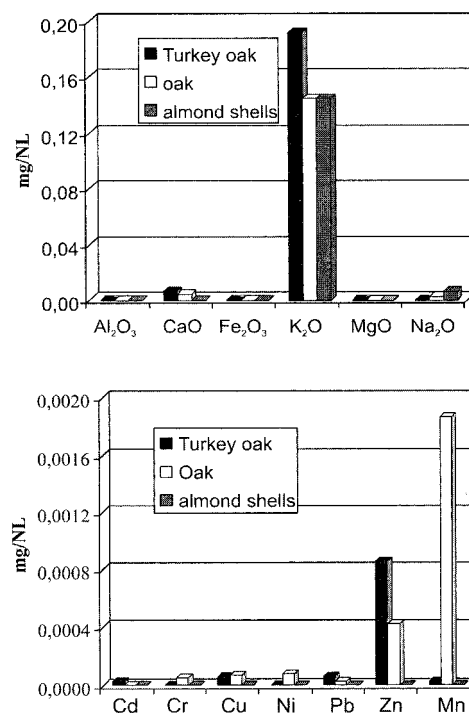

Figure 2. Metals distribution in collected fly ash samples from gasification of woody biomass.

(Owen and Thomas[17]). As already reported by Owen, the intensity measurements were carried out on a base line reference measured by eye for each sample. The ratios estimated with this procedure are comparable to that calculated on the basis of the chemical method.

Inorganic Constituents Composition of the Gas. Figure 2 displays the composition of alkali−alkaline earth and heavy metals in the gas mixture relevant to the three feedstocks. The results seem to be not significantly different. The gas concentrations for heavy and alkali metals indicate that the major amount of inorganic compounds remains at the ash bed in the bottom

(17) Owen, N. L.; Thomas, D. W. Infrared Sudied of Hard and Soft Woods. *Appl. Spectrosc.* **1989**, *43* (3), 451−457.

Table 5. Functional Groups on the Surface of Char Collected during Biomass Gasification

absorption freq (cm^{-1})	assignt[a]
1690	C=O stretch of aromatic acid
1631	C=C stretch
1383	C−O stretching vibrations
1270	C−O−C asymmetric stretching
1120	C−O−C symmetric stretching

[a] Assignment regions are reported in ref 18 and in the refereneds cited therein.

of the gasifier. It is worth noticing that while heavy metals retain almost the same relative distribution to one another in the fly ash with respect to the analyzed composition of the raw biomass, a predominant presence of potassium can be observed in the fly ash. The highest volatility of KCl among the inorganic compound present in the biomass was often restated to explain the potassium presence in the collected fly ash.[18] However, KCl volatilization might not be the only mechanism, proven by the fact that turkey oak feedstocks give fly ash with more potassium than that from oak despite the lower chlorine content. This finding indicates that additional reactions might be invoked. Among others, organic salts such as R−COOK on the surface of char could be precursors of the formation of potassium inorganic species in the fly ash. The FTIR spectrum of a typical char carried in suspension by the gas shows a wide absorption band in the region of 1600 cm^{-1}, where carboxyl−carbonate functionality falls.[19] Table 5 lists characteristic absorption bands recognizable in the FTIR spectrum of a collected char sample with the assignments relevant to the chemical functional groups. Unfortunately, although the reported assignments confirm the presence of oxygenated functionality, they are weak and cannot be considered conclusive, especially in the part of the spectrum containing O−H stretching absorption bands. In fact, as a result of the high hygroscopicity observed for these materials, the presence of water traces is expected. While the features from the acquired FTIR spectra do not vary with the biomass loaded, an approximately 2-fold increase was observed for the char collected from almond shells with respect to woody biomass. This result, which primarily reflects a different percentage of fixed carbon (Table 1) in the tested biomass, can be explained not only in light of a different lignin percentage[20] but also because of the different ash content and composition. More in detail, a higher ash content, especially calcium ions, in woody biomass was already found to be responsible for a higher catalytic effect toward char gasification in a CO_2 atmosphere.[7]

Figure 3 displays the concentrations of acetates and potassium in the flue gas for woody biomass. It seems interesting the fact that the amount of potassium quantified on the quartz filter is comparable to the amount of acetates collected in the anionic sampling
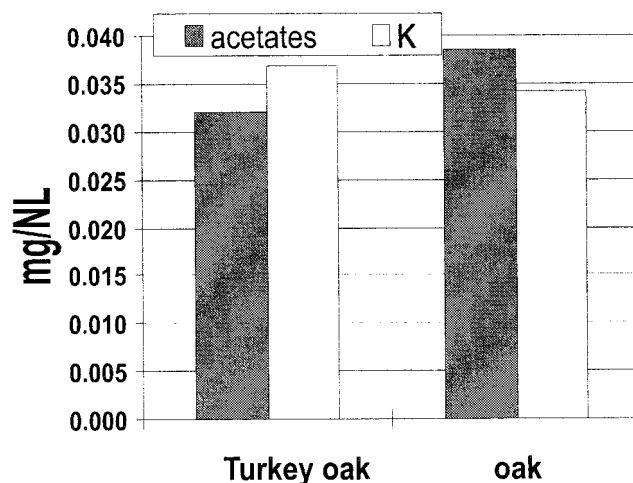
Figure 3. Comparison between acetate and potassium concentrations in the flue gas for woody biomass.
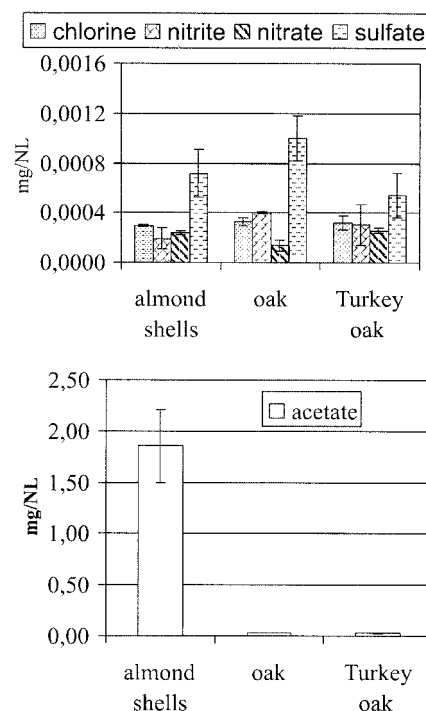
Figure 4. HPLC analysis of the flue gas inorganic composition (chlorine, nitrite, nitrate, sulfate, acetate).

solution. This result suggests a common source in the formation pathway of these species. Some hypotheses about thermal degradation of alkaline carboxylates have already been formulated by Zintl et al.[21] Unfortunately, due to the high concentration of acetic acid detected during the test runs with almond shells, it was not possible to verify the above correlation also in these experiments (vide infra).

Figure 4 displays the measured gas composition for some anions of interest. The reported errors were computed on the number of the test runs. It is apparent that while no significant differences exist among the examined biomass for the concentration of chlorine,

(18) Kaufmann, H.; Nussbaumer, T. Characteristic and Formation of Fly Ash Particles in Biomass Furnaces. In *Biomass for Energy and Industry, Proceedings of the International Conference Würzburg*; Kopetz, H., Weber, T., Palz, W., Chartier, P., Ferrero, G. L., Eds.; C.A.R.M.E.N.: Germany, 1998; pp 1327−1329.

(19) Fanning, P. E.; Vannice, M. A. A Drift Study of the Formation of Surface Groups on Carbon by Oxidation. *Carbon* **1993**, *31*, 721−730.

(20) Zanzi, R.; Sjostrom, K.; Bjornbom, E. Rapid high-temperature pyrolysis of biomass in a free-fall reactor. *Fuel* **1996**, *75*, 545.

(21) Zintl, F.; Stömberg, B.; Björkman, E. Release of chlorine from biomass at gasification conditions. In *Biomass for Energy and Industry, Proceedings of the International Conference Würzburg*; Kopetz, H., Weber, T., Palz, W., Chartier, P., Ferrero, G. L., Eds.; C.A.R.M.E.N.: Germany, 1998; pp 1608−1611.
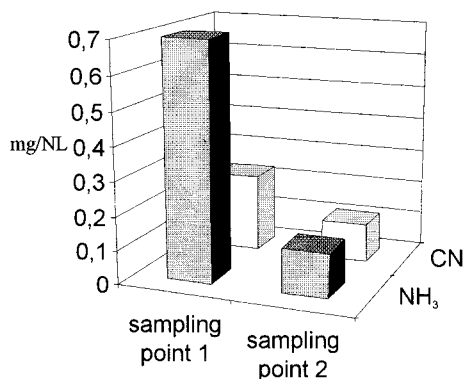
Figure 5. Comparison between the ammonia and cyanide concentrations in the flue gas at sampling points 1 and 2 (SP1 and SP2, respectively, of Scheme 1).

nitrites, nitrates, and sulfates in the flue gas, the concentration of acetates in the flue gas from almond shells is 60-fold that from woody biomass. Measures of pH in the water phases condensed on the dichloromethane during the tar sampling step confirm the predominance of the acidic constituents in the flue gas from almond shells. More exactly, water phases from almond shells have pH 5, while the ones from woody biomass have about pH 9. A reasonable explanation for this difference could be the different distribution of the holocellulose constituents already discussed on the basis of the results listed in Table 3. In particular, the highest content of xylan in almond shells can justify the difference in the measured acetic acid concentration in the flue gas from the two different feedstocks considering that xylanes in hemicellulose are acetylated in the O−2 position. This experimental result corroborates the theory proposed by Evans and Milne[22] to explain the presence of acetic acid in the mass spectral patterns relevant to the biomass pyrolysis products.

In the analysis of products distribution from gasification processes, attention must be devoted to the study of inorganic nitrogen compounds in the flue gas because of the problems connected with their burning. In fact, it is evident from Figure 5 that only a small part of the ammonia contained in the flue gas was removed by the wet scrubber before entering the chips filter section. The analysis of water phase condensed on the chips filter confirmed the presence of an appreciable amount of ammonia.

Figure 6 provides the ammonia and cyanide concentration in the flue gas as a function of the gasification ratio for the two woody biomass and almond shells. Data reported make evident that ammonia evolution from the two biomass classes is different. Less pronounced differences can be observed in the cyanide trends. In particular, the ammonia concentration for almond shells is almost 2-fold that for the two woody biomasses at the same gasification ratio. To investigate the relation between the nitrogen content of the tested biomass and the amount of ammonia produced during the gasification process, the elemental analysis was performed (Table 1). As expected, data obtained show that the nitrogen percentage in almond shell feedstocks is 4-fold

that in woody feedstocks. On the basis of these results, it can be concluded that ammonia evolution is primarily affected by the amount of nitrogen in the loaded feedstock, although the evaluated percentage conversion of the fuel−nitrogen is below 1%. Besides this information, Figure 6 also indicates that ammonia and cyanide concentrations in the flue gas are also influenced by the gasification ratio, to say they are influenced by the relative amount of air (oxygen) injected into the gasifier with respect to the loaded biomass. It is worth noting that while ammonia concentration increased with the increasing of the gasification ratio, the cyanide concentration dropped to zero in a comparable range of values. This behavior could be explained by the oxidation of cyanide by molecular oxygen in air,[23] taking into account that the presence of woody charcoal and copper species in the same reaction medium can make this thermodynamic oxidation kinetically possible. The potential reaction pathways are reported below:

$$2CN^- + O_2 = 2CNO^-$$

$$2CNO^- + {}^3/_2O_2 + H_2O = N_2 + 2CO_2 + 2OH^-$$

$$CNO^- + 2H_3O^+ = CO_2 + NH_4^+ + H_2O$$
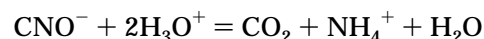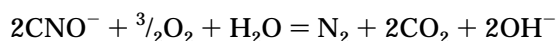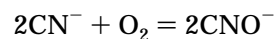
Measures of BET isotherm were carried out to explore if the gasification conditions are effective toward a certain activation of the woody charcoal so making it possible the described reactions. Table 6 displays the measured surface area for the charcoal introduced in the gasifier necessary to burn the biomass in the starting up stage and the charcoal at the end of a typical plant running. The comparison between the reported results suggests that, at the operating conditions selected for the test runs, an appreciable increase of about 1 order of magnitude of the charcoal surface area has been observed

Comparing the results of this study with that reported by Leppälahti et al.[12] for gasification of wood in updraft fixed bed gasifiers, some valuable differences can be outlined. In particular, data collected from the updraft gasifier showed a higher percentage conversion of fuel nitrogen both in the case of ammonia and cyanide formation. This result is coherent with the downdraft gasifier geometry that provides the passage of ammonia and cyanide species over the ash bed in the boiler where certain decomposition reactions can be favored from the presence of inorganic species such as CaO, MgO, and NiO.

Tar Content and Composition in the Gas. Figure 7 provides a typical chromatogram for a tar sample, while in Table 7 the detected and quantified constituents of the three biomass feedstocks are listed. It is evident from the reported amounts that toluene and its derivative compounds such as xylene are the most abundant constituents followed by phenol, naphthalene, and traces of polyaromatic hydrocarbons. Moreover, tar composition does not exhibit appreciable amounts of nitrogen derived compounds in the cases of both woody biomass and almond shells. For a better illustration of the changes in the distribution of tar constituents in

(22) Evans, R. J.; Milne, T. A. Molecular Characterization of the Pyrolysis of biomass. 1. Fundamentals. *Energy Fuels* **1987**, *1*, 123−137.

(23) Chen, Y. You, C. Cyanide Destruction by Catalytic Oxidation. *Metal Finishing* **1991**, *89* (11), 68−71.
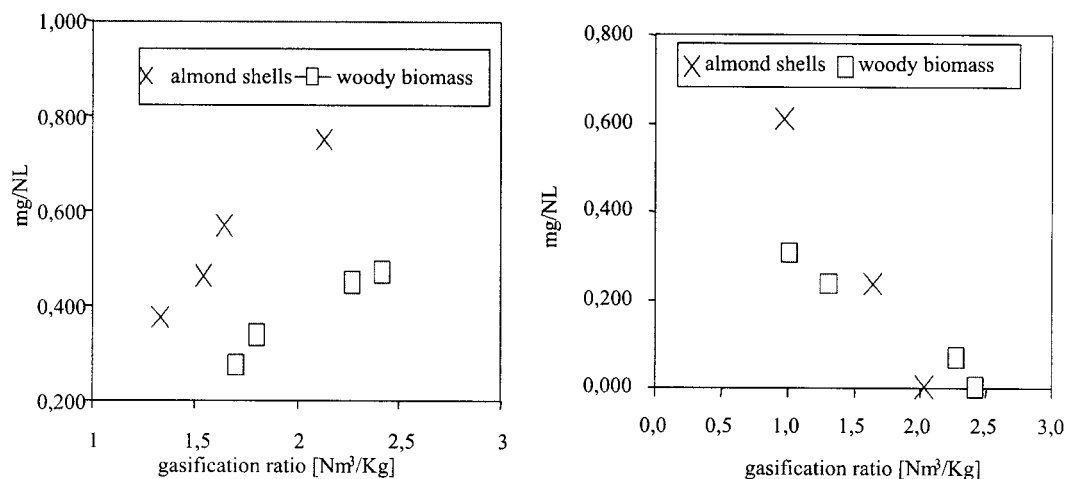
Figure 6. Ammonia and cyanide concentrations in the flue gas from woody biomass and almond shells versus gasification ratio. Note that the reported concentrations for ammonia and cyanide species do not correspond to the same sampling.

Table 6. Measured Surface Areas (m^2/g)

	surface area
charcoal introduced in the gasifier	16
charcoal at the end of the process	110

Table 7. Mean Percentage Compositions of the Identified Tar Constituents for Almond Shells, Oak, and Turkey Oak[a]

compd	almond shells	oak	turkey oak
(1) toluene	41.29	46.07	62.46
(2) ethylbenzene	22.71	10.52	10.71
(3) *p*-xylene	4.24	7.73	5.74
(4) styrene	27.86	32.56	18.16
(5) phenol	1.32	0.35	0.19
(6) indene	0.10	0.41	traces
(7) *o*-cresol	0.56	0.07	traces
(8) *p*-cresol	1.04	0.19	traces
(9) naphthalene	0.38	1.06	1.72
(10) 1-methylnaphthalene	traces	0.16	traces
(11) 2-methylnaphthalene	traces	0.11	traces
(12) acenaphthylene	0.12	0.38	0.32
(13) acenaphthene	traces	traces	traces
(14) fluorene	traces	traces	traces
(15) phenantrene	traces	0.15	0.25
(16) anthracene	traces	traces	traces
(17) fluoranthene	traces	traces	0.13
(18) pyrene	traces	traces	0.19

[a] From the chromatogram, typical variances within-sample were about 5% for the more abundant compounds (benzene and naphthalene types) and about 15−20 for the trace constituents. The estimated variance between runs was typically not more than 20%.
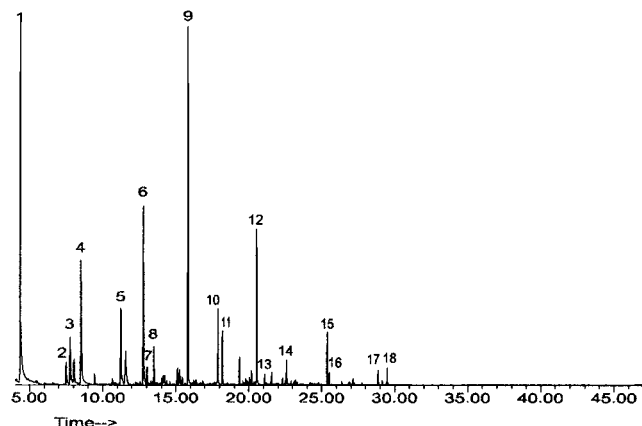

Figure 7. GC-MS chromatogram of tar species collected on a CH_2Cl_2 solution during a gasification of oak biomass.
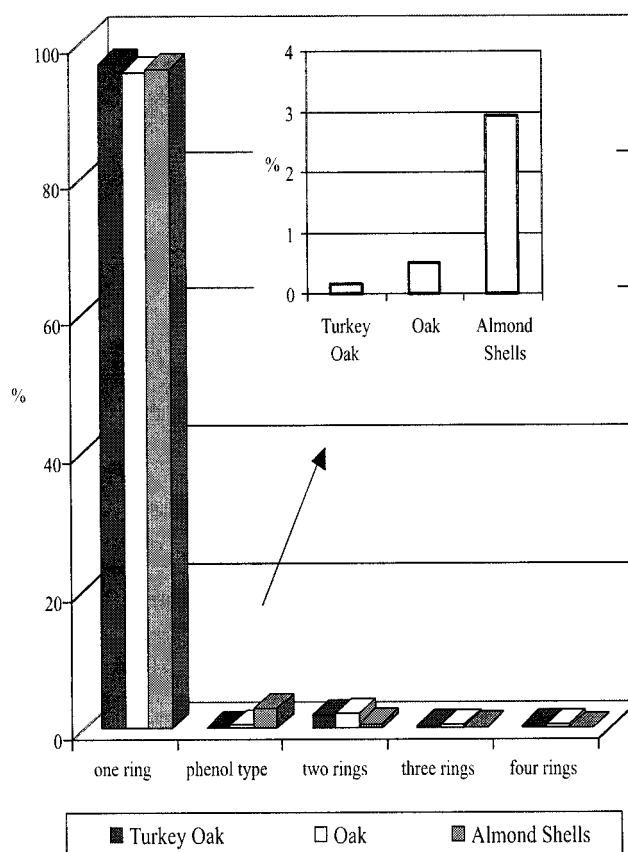

Figure 8. Relative distribution of tar compounds grouped into four principal classes: one ring type (toluene, ethylbenzene, xylenes, and styrene), phenol type (phenol and cresols), two rings type (naphthalene, 1-methylnaphthalene, 2-methylnaph-thalene, and indene), three rings type (phenanthrene, an-thracene, acenaphthylene, acenaphthene, and fluorene), and four rings type (fluoranthene and pyrene).The insert magnifies the phenol compounds region of the istogram.

the three biomass feedstocks, the quantified compounds were divided into four classes: one ring compounds, phenol and phenol type compounds, two and three rings compounds (Figure 8). Results show that woody biomass and almond shell tar compositions differ only in the relative percentage of phenol and phenol type com-pounds. The magnification displayed in Figure 8 enables this difference to emerge. This result is coherent with
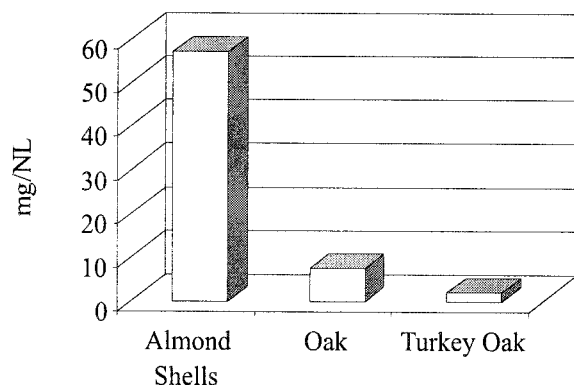
Figure 9. Comparison among the total amount (mg/NL) of tar from oak, turkey oak, and almond shells.

the pattern observed in the lignin content (Table 4). More pronounced differences in tar produced from the three biomass feedstocks are evident in Figure 9, where the total amounts of produced tar for the tested biomass are compared. Here, the amount of collected tar from almond shells is almost 10-fold that from woody biomass. These results could be tentatively explained by the catalytic activity of the indigenous alkaline earth metals such as calcium toward the cracking of high molecular tar in view of their activity in catalysts such as dolomite and calcite. In particular, at the gasifier running temperature of 850 °C, inorganic species such as calcium and magnesium in the biomass feedstock are likely to be present as CaO and MgO, to stay in the active form to catalyze tar cracking. Considering that woody composition is richer in calcium content than almond shells, the woody fuel could be subjected to a cracking operated by indigenous catalysts. Also it cannot be excluded that a different content in the lignin component might have affected the amount of produced tar. In fact, besides the fact that the lignin backbone could be a source of phenol compounds for the produced tar, it is well-known that in the biomass matrix it plays the role of linking agent for the holocellulose component. A major amount of lignin can account for a more difficult defiberization process of the biomass in the process starting up. In

particular, a major amount of lignin could make the holocellulose backbone less available in the pyrolysis zone causing a higher uncombusted partially cracked product flow from the combustion to the reduction zone of the gasifier itself.

Characterization of Sludgy Material. Figure 10 displays the FT-IR spectrum of a typical sludge sample that tends to condense in the upper part of the gasifier during the earlier phases of the process. The collected spectrum looks similar to a typical spectrum from a lignin sample so confirming the existence of a defiberization step in the gasification process during which some fragments of lignin remain unaltered.

Gasification Rate. Figure 11 reproduces the diminution of the biomass feedstock loaded as a function of the time. The reported slopes for the three biomasses investigated are a measure of the gasification rates. The comparison of the reported values suggests that the gasification of almond shells is slower than that of woody biomass. This result is different from that expected on the basis of the fact that almond shells are smaller than woody material and, thanks to a major uniformity of the temperature in the reaction zone of the gasifier, they should gasify more quickly. Also in this case the different amount of lignin measured in the two analyzed feedstocks could explain the observed difference. In particular, a different lignin percentage is likewise reflected in the biomass morphology. In fact, almond shells have a morphology harder than wood other than less porous. Detailed examination of the inorganic composition listed in Table 2 seems to indicate that if alkali and alkaline earth metals play a role in determining the gasification rate, calcium is the more effective species. This result agrees with the bench experiments run by DeGroot and Richards,[7] while it does not match perfectly data reported from some authors[24,25] in the study of other carbonaceous materials about the potassium reactivity. The gained information confirms that the inorganic content of the biomass cannot explain at all the observed phenomena and that it must be inserted in the context of a complete structural analysis of the substrate. Other investiga-
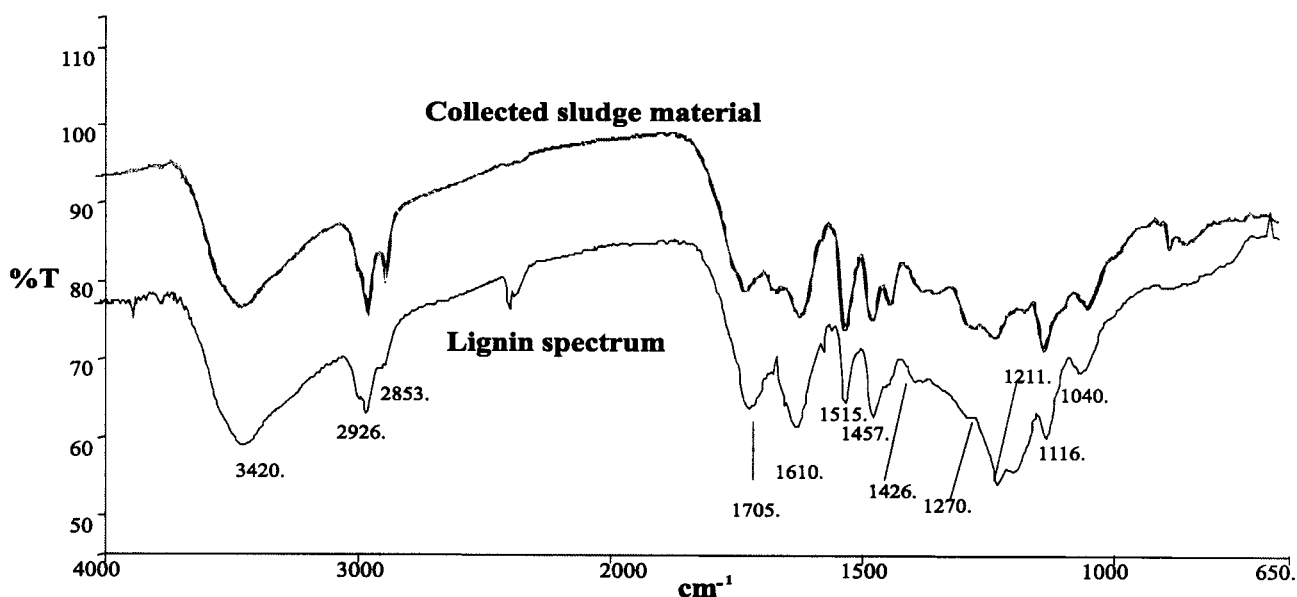

Figure 10. FT-IR spectrum relevant to gasification products condensed in the upper part of the gasifier.
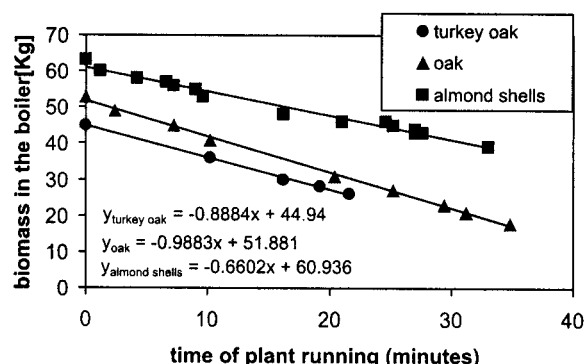
Figure 11. Rate of biomass consumption during a gasification process.

tions are currently progressing to extend these studies to other biomass feedstocks.

Conclusions

A pilot plant for fixed bed gasification of biomass is being operated at the ENEA Researcher Centre of Trisaia (Italy). A detailed survey of both inorganic and organic compositions of the flue gas was carried out. The difference observed under similar conditions in the product distribution from the gasification of the three different biomass feedstocks are interpreted in light of interactions between the organic backbone and the inorganic constituents of the tested materials.

The following conclusions are drawn:

1. The composition of the tested biomass feedstocks shows significant differences with regard to both organic and inorganic constituents. The analysis of the metal compositions reveals that, among the main con-

stituents, the woody biomass is richer in calcium than almond shells while poorer with regard to the potassium concentration. Interesting differences have also been recorded in the distribution of the minor constituents. The analysis of the organic matrix compositions indicates that woody biomass has lower percentages of both xylan units and lignin content than almond shells.

2. There are at least three important roles that might be assigned to calcium toward the gasification process: (i) to operate a certain decomposition of ammonia, (ii) to promote an internal cracking of the produced tar, and (iii) to catalyze char gasification.

3. Different lignin percentages in the biomass feedstocks are reflected in different phenol concentrations in the flue gas and in different gasification rates.

4. The high percentage of xylan units from almond shell feedstocks with respect to woody ones are found to be associated with a higher acetic acid concentration in the flue gas.

Some other evaluations have been carried out by studying the dependence of the products distribution as a function of the gasification ratio. In this regard, oxygen was found to increase the amount of ammonia in the flue gas while decreasing that of cyanide. A reaction pattern was proposed to explain the observed trends.

(24) Chen, S. G.; Yang, R. T. The active surface species in alkali-catalyzed carbon gasificatio: Phenolate (C-O-M) groups vs clusters (particles). *J. Catal.* **1993**, *141*, 102−113.

(25) Chen, S. G.; Yang, R. T. Mechanism of alkali and alkaline earth catalyzed gasification of graphite by CO_2 and H_2O studied by electron microscopy. *J. Catal.* **1992**, *138*, 12−23.